Weak-layer spatial variability as a possible trigger of slab tensile failure

Johan Gaume[1,*], Guillaume Chambon[2], Nicolas Eckert[2], Mohamed Naaim[2]
[1] WSL Institute for Snow and Avalanche Research SLF, Davos, Switzerland
[2] IRSTEA, Grenoble, France

ABSTRACT: The evaluation of the location of slab tensile failure represents an important concern for the evaluation of the extent of avalanche release zones and hence hazard assessment. In this study, a mechanically-based statistical model of the slab-weak layer system accounting for weak-layer spatial variability, stress redistributions by elasticity of the slab and the slab possible tensile failure is simulated using a stochastic finite element method. Two types of avalanche releases are distinguished in the simulations: (1) full slope releases, for which the entire simulated slope is released and the heterogeneity is not sufficient to trigger a tensile failure within the slab; (2) partial slope releases, for which tensile failure occurs within the slab due to the heterogeneity so that only a part of the slope is released. We present the proportion of these two release types as a function of the different model parameters obtained from finite element simulations. One of the main outcomes is that, for slab tensile strength higher than the average cohesion of the weak layer, all the releases appear to be full-slope, justifying the major influence of topographical and morphological features such as rocks, trees, slope curvature, ridge and heterogeneous snow cover often claimed in the literature.

KEYWORDS: Snow avalanche, avalanche release, slab, weak layer, spatial variability, tensile failure.

1 INTRODUCTION

Avalanche hazard mapping procedures have seen the growing popularity of coupled statistical-deterministic models in order to evaluate runout distance and maximal pressure distributions at any location of the runout zone (Barbolini et al., 2000; Naaim et al., 2003; Ancey et al., 2004, Eckert et al., 2007a; Eckert et al., 2008 and Eckert et al., 2010). These coupled models require the release volume as input, combination between the release depth and area. Concerning the evaluation of the release depth, empirical techniques already exist (Swiss guidelines: Salm et al., 1990) and more recently, a coupled statistical-mechanical model has been proposed by Gaume et al., (2012, 2013) taking into account both mechanical and meteorological factors in a probabilistic framework.

On the other hand, the position and the extent of the release zone have been little investigated. Maggioni et al., (2002) and Maggioni and Gruber, (2003) analyzed a well-documented database of avalanche events with respect to several topographic characteristics and showed that the mean slope angle, the curvature and the distance to the ridge are the most important parameters influencing the distribution of the avalanche release. Failletaz et al., (2006), Fyffe and Zaiser, (2004, 2007) used cellular-automata approaches to compute avalanche release area distributions. These models include a source of stochastic variability such as the heterogeneity of weak layer mechanical properties. Interestingly, these models are capable, under certain conditions, to reproduce the power-law area distributions observed from field measurements (McClung, 2003, Failletaz et al., 2004).

Our aim is to extend a mechanically-based probabilistic model developed in a previous study (Gaume et al., 2012, 2013) to analyze the parameters influencing the position of the slab tensile failure and, hence, the extent of the release area.

In a first section, we recall the main characteristics of the model and present the changes made compared to its previous versions. Then, in the second section, two rupture types are distinguished and presented. Finally, in the third section, we quantify the influence of weak layer heterogeneity and slab tensile strength on the position of slab tensile failure.

2 PRESENTATION OF THE MODEL

In this study, the mechanically-based statistical model proposed by Gaume et al., 2013 is used. We recall here its main characteristics.

The simulated system is a uniform slope composed of a slab and a weak layer of length L= 50 m. The simulations are carried out using the finite element code Cast3m in 2D (plane stress condition). Gravity is the only applied external force and the system is loaded by pro-

Corresponding author address: Johan Gaume, WSL Institute for Snow and Avalanche Research SLF, Flüelastrasse 11, CH-7260 Davos Dorf, Switzerland;
tel: +33 6 748 23 547;
email: gaume@slf.ch

gressively increasing the slope angle θ until rupture. The main change compared to Gaume et al., 2013's model concerns the constitutive law of the slab. In order to take into account the possible tensile failure of the slab, we use here an elastic-brittle law. The Young modulus of the slab is E = 1 MPa, the Poisson ratio ν = 0.2, and the density ρ =250 kg.m^{-3}. The tensile strength of the slab is denoted σ_T and was varied between 500 and 2000Pa.The weak layer is modelled as a quasi-brittle (strain-softening) interface with a
Mohr-Coulomb rupture criterion characterized by a cohesion c and a friction coefficient μ =tan30°. A spatial heterogeneity of the weak layer is accounted for through a stochastic distribution of the cohesion c with a spherical covariance function of correlation length ε. The average cohesion is denoted $< c >$and its overall standard deviation σ_c.

Besides the evaluation of avalanche release depth distributions, this model enabled to evidence, a heterogeneity smoothing effect caused by stress redistribution due to slab elasticity and characterized by the ratio between correlation length ε and a typical length scale of the system associated to elastic effects (see Gaume et al., 2012, 2013).

3 RELEASE TYPES

Two types of avalanche releases were distinguished in the simulations:

(1) full slope release, for which the entire simulated slope is released without tensile failure within the slab (Fig. 1a);

(2) partial slope release, for which tensile failure occurs within the slab so that only a part of the slope is released (Fig. 1b).

Importantly, however, for both release types, the primary rupture process observed is always the shear failure of the weak layer. Slab rupture, when existent, systematically constitutes a secondary process. In the case of a full slope release, the heterogeneity magnitude is not sufficient to trigger a tensile failure within the slab. The basal shear failure in the weak layer thus propagates until the top boundary condition which can be seen as an anchor point or a zone of high concentration of tensile stresses where slab tensile failure would occur (Fig. 1a). Replaced in the context of natural avalanche paths, this boundary condition can represent a strong morphological feature susceptible to trigger the tensile failure (ridges, rocks, trees, local convex zone, etc.).

On the contrary, for partial slope releases, the cohesion variations in the weak layer are sufficient to generate the tensile failure within the system. Local strong zones can effectively stop the progression of the basal failure and the excess of stress is redistributed in the slab which engenders slab tensile opening.

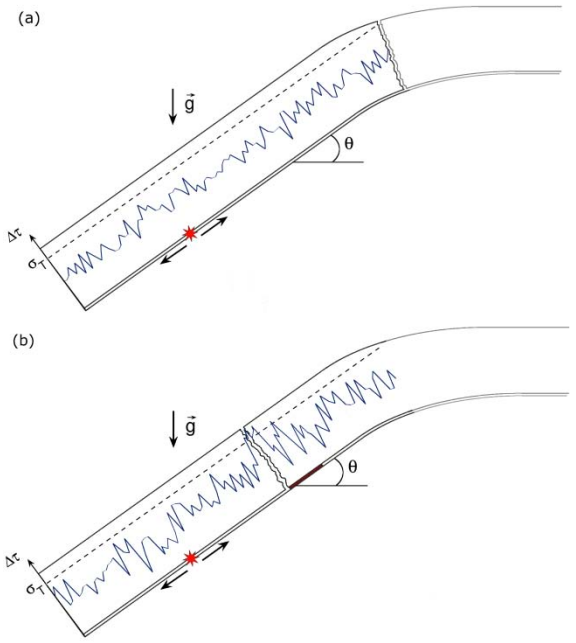

Figure 1. Diagram representing the two types of failure observed in the simulations. (a) full-slope release: the position of the slab tensile failure is influenced by morphological features (rocks, trees, ridge, curvature...). (b) partial-slope release: the local heterogeneity is sufficient to trigger the tensile failure within the slab. The red-colored part of the weak layer represents a local zone of important shear strength. The blue curves represent an illustration of the heterogeneity of shear stress difference between two adjacent elements $\Delta\tau$ and the dotted line represents the tensile strength σ_T.

4 RESULTS

In this section, we present the results in terms of partial slope release probability, also called tensile failure probability and denoted P_{tf}, as a function of the following model parameters: tensile strength σ_T correlation length ε, slab depth h. In a first step, the average cohesion and the standard deviation are kept fixed ($< c >$=1kPa, σ_c=300Pa).

4.1 Influence of the tensile strength

Fig. 2 represents the probability of tensile failure P_{tf} within the system as a function of the tensile strength σ_T for different values of the correlation length ε and a constant slab depth h=1m. Tensile strength values are varied between 0.5 and 1.5kPa. As expected, this probability decreases with the tensile strength σ_T from 100% to 0%. The rate of decrease and

tensile strength values at 0 and 100% depend on the correlation length ε.

4.2 Influence of the correlation length

The influence of correlation length ε is also noticeable on Fig. 2. The higher ε is, the slower the probability decreases with σ_T. Besides, for constant tensile strength values, P_{tf} globally decreases with ε. The values of σ_T for P_{tf} =100% is decreasing with increasing correlation length while the value for P_{tf} =0% is almost not affected by ε.

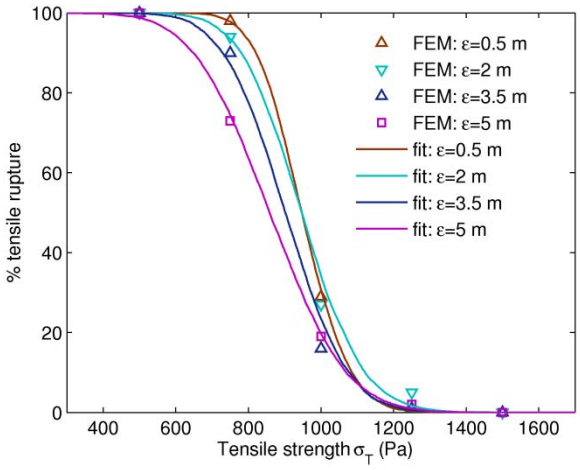

Figure 2. Probability of slab tensile failure P_{tf} within the simulated system (partial-slope release) as a function of the tensile strength σ_T for different values of ε and a constant slab depth h=1m representing the two types of failure observed in the simulations. The curves represent the adjustment given by the statistical model presented in Sec. 5.

4.3 Influence of the slab depth

Fig. 3 reports the tensile failure probability P_{tf} as a function of h for different tensile strength values and a constant correlation length ε=0.5m. For σ_T < 0.75kPa, P_{tf} is approximately equal to 100%, whereas, P_{tf} is approximately equal to 0% for σ_T > 1.5kPa. For intermediate values of σ_T, P_{tf} decreases from h=0.5m to h=2m. A single simulation for h=0.25m was also performed for σ_T =1kPa to confirm the increase of P_{tf} with h for h < 0.5m that will be highlighted be the statistical model developed in the next section.

5 A SIMPLE STATISTICAL MODEL

In order to estimate the proportion between the two release types, one can define the probability that the tensile stress σ_{xx} in the slab exceeds the tensile strength σ_T. We have shown that, a necessary condition for slab release is the primary rupture in shear of the weak layer.

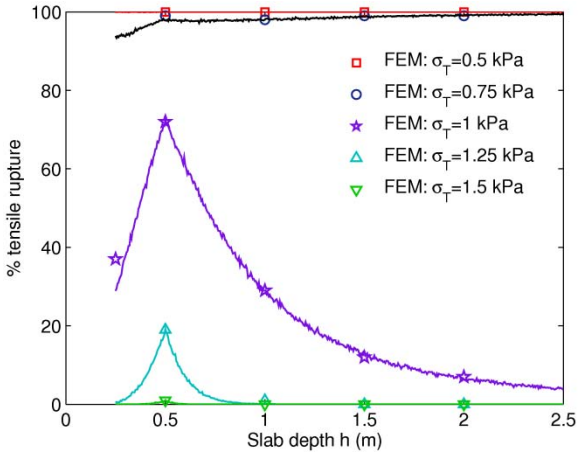

Figure 3. Probability of slab tensile failure P_{tf} with the simulated system (partial-slope release) as a function of slab depth h for different values of the tensile strength σ_T and a constant correlation length ε=0.5m. The curves represent the adjustment given by the statistical model presented in Sec. 5.

Thus, this probability $P(\sigma_{xx} > \sigma_T)$ is assumed to be equal to $P(\Delta\tau > \sigma_T)$, the probability that the shear stress difference $\Delta\tau$ between two adjacent elements of the weak layer exceeds the tensile strength σ_T. The shear stress difference $\Delta\tau$ is due to weak layer cohesion heterogeneity. Because of the Gaussian character of weak layer heterogeneity, we assume that $\Delta\tau$ also follows a Gaussian law of average $<\Delta\tau>$ and standard deviation $\sigma_{\Delta\tau}$.

With this last assumption, one can compute the exceedence probability $P(\Delta\tau > \sigma_T)$ analytically. It is given by:

$$P(\Delta\tau > \sigma_T) = 1 - \frac{1}{2}\left[1 + \mathrm{erf}\left(\frac{\sigma_T - <\Delta\tau>}{\sqrt{2}\sigma_{\Delta\tau}}\right)\right] \quad (1)$$

This equation was adjusted to the finite element results, namely to the evolution of P_{tf} with σ_T for different values of ε (Fig. 2, continuous lines) and to the evolution of P_{tf} with σ_T for different values of h (not represented). The two parameters $<\Delta\tau>$ *and* $\sigma_{\Delta\tau}$ where thus evaluated as a function of h and ε. Consequently, this model enables to predict the proportion between the two observed types for all values of the parameters. For instance, we represented on Fig. 3 as continuous lines, the complete evolution of this proportion for different slab depth values. The agreement with FEM datapoints is excellent. Notably, the model was calibrated using only values of h > 0.5m. Hence, the increase of P_{tf} between 0 and 0.5m was first predicted by the model, and later confirmed by an additional FEM simulation conducted for h=0.25m.

As a consequence, we argue that this simple model can reproduce with a good accuracy the

relative proportion of full and partial slope releases.

6 DISCUSSION & CONCLUSIONS

We presented two different release types observed in our simulations. (1) Full-slope releases are influenced by the morphology of the path and/or snow-cover variations since the heterogeneity is not sufficient to trigger a tensile failure. For instance, the tensile failure will be very sensitive to the presence of trees, rocks, ridges and local curvature. (2) Partial-slope releases for which the local variations of weak-layer cohesion are substantial and can trigger the slab tensile crack on their own. Importantly, for both release types, the primary rupture process observed is always the basal shear failure of the weak layer. Hence slab rupture systematically constitutes a secondary process.

We have shown that the proportion between these two types is extremely dependent on the model parameters such as the tensile strength σ_T, the slab depth h, the correlation length ε, and most probably on other parameters that have not been varied in this study such as the average cohesion $< c >$ and the cohesion standard deviation σ_c. Besides, we presented a simple statistical model capable of reproducing the proportion between release types as a function of the model parameters. Two illustrations of this simple model are represented on Fig. 1. In the first case (Fig. 1a), the shear stress difference $\Delta\tau$ is always lower than the tensile strength σ_T. The basal failure thus propagates over the entire system until the top boundary condition which is a zone of high concentration of tensile stresses. This zone can be seen as a ridge, a rock, a tree or a local curvature. In the second case (Fig. 1b), a local zone of substantial shear stress difference $\Delta\tau$ due to strong variations of the cohesion generates a local tensile failure within the slab since $\Delta\tau > \sigma_T$.

We have shown that for values of σ_T higher than the average cohesion $< c >$=1kPa (in this case) the releases are almost always full slope and consequently they are controlled by the morphology of the path. Let us recall that tensile strength values from laboratory tests appear to be globally higher than 1kPa (Jamieson and Johnston 1990, Sigrist 2006) according to many different measurement techniques whereas shear strength values of weak layers are typically lower than 1kPa. This indicates, for realistic values of the mechanical parameters, the major influence of slope morphology and topography on the position of the slab tensile failure and thus on the extent of the release area. This effect is further amplified when the slab depth is high compared to the correlation length and elasticity tends to smooth out the heterogeneity influence. Such a conclusion corroborates and

Figure 4. Diptych: Avalanche triggered by a snowboarder. The release area is defined by the ridge at the crown and rock and trees at flanks. Left side: before the impact of the snowboarder. Right side: after the impact. © Rémi Petit.

brings some mechanical justification to the results found by Maggioni and Gruber 2003 who analyzed the influence of morphological features of the path on the extent of the release area using a purely data-driven statistical approach, and concluded that local geometry plays a dominant role in the location and extent of avalanches.

Hence, in practice, the release area is mainly dependent on slope topography (local curvature, ridge, etc.), or on the presence of rocks and trees for instance. For example, Fig. 4. shows a typical slab avalanche release area defined by the ridge at the crown and by rocks and trees at flanks.

7 REFERENCES

Ancey, C., C. Gervasoni and M Meunier, 2004. Computing extreme avalanches, Cold Reg. Sci. Technol., 39, 161–180.

Barbolini, M, U Gruber, C Keylock, M Naaim and F Savi, 2000. Application and evaluation of statistical and hydraulic-continuum dense-snow avalanche models to five real European sites, Cold Reg. Sci. Technol., 31(2), 133–149.

Eckert, N, M Naaim and E. Parent, 2010. Long-term avalanche hazard assessment with a Bayesian depth-averaged propagation model, J. Glaciol., 56(198), 563–586.

Eckert, N., E. Parent, M Naaim and D. Richard, 2008. Bayesian stochastic modelling for avalanche predetermination: from a general system framework to return period computations, SERRA, 22, 185–206.

Eckert, N, E. Parent and D. Richard, 2007. Revisiting statistical topographical methods for avalanche predetermination: Bayesian modelling for runout distance predictive distribution, Cold Reg. Sci. Technol., 49(1), 88–107.

Failletaz, J, F Louchet and J.R Grasso, 2004. Two-threshold model for scaling laws of noninteracting snow avalanches, Phys. Rev.Lett., 93(20), 208001.

Failletaz, J, F Louchet and J.R Grasso, 2006. Cellular automaton modelling of slab avalanche triggering mechanisms : from the universal statistical behaviour to particular cases, Proceedings of the ISSW, 174-180.

Fyffe, B and M Zaiser, 2004. The effects of snow variability on slab avalanche release, Cold Reg. Sci. Technol., 40, 229–242.

Fyffe, B and M Zaiser, 2007. Interplay of basal shear fracture and slab rupture in slab avalanche release, Cold Reg. Sci. Technol., 49, 2638.

Gaume, J., G. Chambon, N. Eckert and M. Naaim, 2013. Influence of weak-layer heterogeneity on snow slab avalanche release: Application to the evaluation of avalanche release depths., J.Glaciol., 59(215), 423-437

Gaume, J., G. Chambon, N. Eckert and M. Naaim, 2012. Relative influence of mechanical and meteorological factors on avalanche release depth distributions., Geophys. Res. Lett., 39, L12401

Jamieson, B and C Johnston, 1990. In-situ tensile tests of snowpack layers, J. Glaciol., 36(122), 102–106.

Maggioni, M. and U Gruber, 2003. The influence of topographic parameters on avalanche release dimension and frequency, Cold Reg. Sci. Technol., 37, 407–419.

Maggioni, M., U. Gruber and M. Stoffel, 2002. Definition and characterisation of potential avalanche release areas, Proceedings of the ESRI Conference, San Diego.

McClung, D.M., 2003. Size scaling for dry snow slab release, J. Geophys. Res., 108(B10), 2465–2477.

Naaim, Mohamed, T Faug and F Naaim-Bouvet, 2003. Dry granular flow modelling including erosion and deposition, Surveys in Geophysics, 24, 569–585.

Salm, B., A. Burkard and H. Gubler, 1990. Berechnung von fliesslawinen: eine anleitung fr pratiker mit beispielen, Internal report EISLF (in German), 47.

Sigrist, C, 2006. Measurements of fracture mechanical properties of snow and application to dry snow slab avalanche release, (PhD thesis), ETHZ.